SUPPORTING INFORMATION

Inverse Thermoreversible Mechanical Stiffening and Birefringence in a Methylcellulose/Cellulose Nanocrystal Hydrogel

Ville Hynninen,[†] *Sami Hietala,*[§] *Jason R. McKee,*[⊥] *Lasse Murtomäki,*[//] *Orlando J. Rojas,*[†‡] *Olli Ikkala*[†‡]*, and *Nonappa,* [†‡]*

† Department of Applied Physics, School of Science, Aalto University, P.O. Box 15100, FI-00076, Espoo, Finland

§ Department of Chemistry, University of Helsinki, P.O. Box 55, FI-00014 HY, Helsinki, Finland

⊥ Betulium Ltd, Tekniikantie 2, FI-02150, Espoo, Finland

// Departments of Chemical and Metallurgical Engineering and Chemistry & Materials Science, School of Chemical Engineering, Aalto University, P.O. Box 16300, FI-00076 Espoo, Finland

‡ Department of Bioproducts and Biosystems, School of Chemical Engineering, Aalto University, P.O. Box 16300, FI-00076 Espoo, Finland

Experimental: Estimating molarity of CNC dispersions for ITC

The mass and molarity of CNC were approximated based on the assumption that one cotton cellulose microfibril consists of 12 * 12 cellulose chains resulting in 144 cellulose chains per microfibril.[1] Based on determined CNC average length (181 nm) by TEM and estimated glucose unit size of 0.5 nm, each cellulose chain in a CNC consists of 362 anhydroglucose units (MW 162 g/mol). Thus, the molecular weight of a single cellulose chain is approximately 58 600 g/mol and the mass of a mol of CNCs is ~8 400 000 g/mol. Calculated from these values the estimated molarity of the used 0.45 wt % CNC dispersion was 0.5 µM (4.5 g/l / 8 400 000 g/mol).

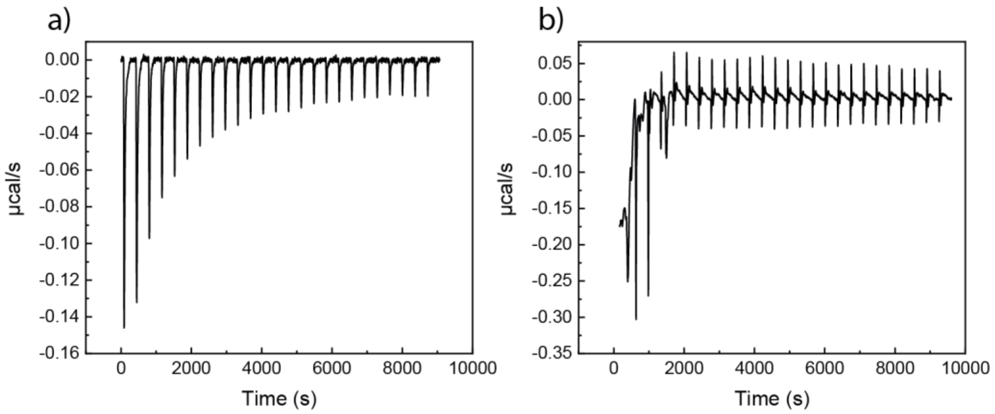

Figure S1. Representative baseline titration graphs measured for ITC at 25 °C. In (a) 0.45 wt % CNC dispersion was titrated into pure water and in (b) pure water into 0.05 mM MC88 dispersion. CNC-to-water baseline was used in analyzing the ITC results.

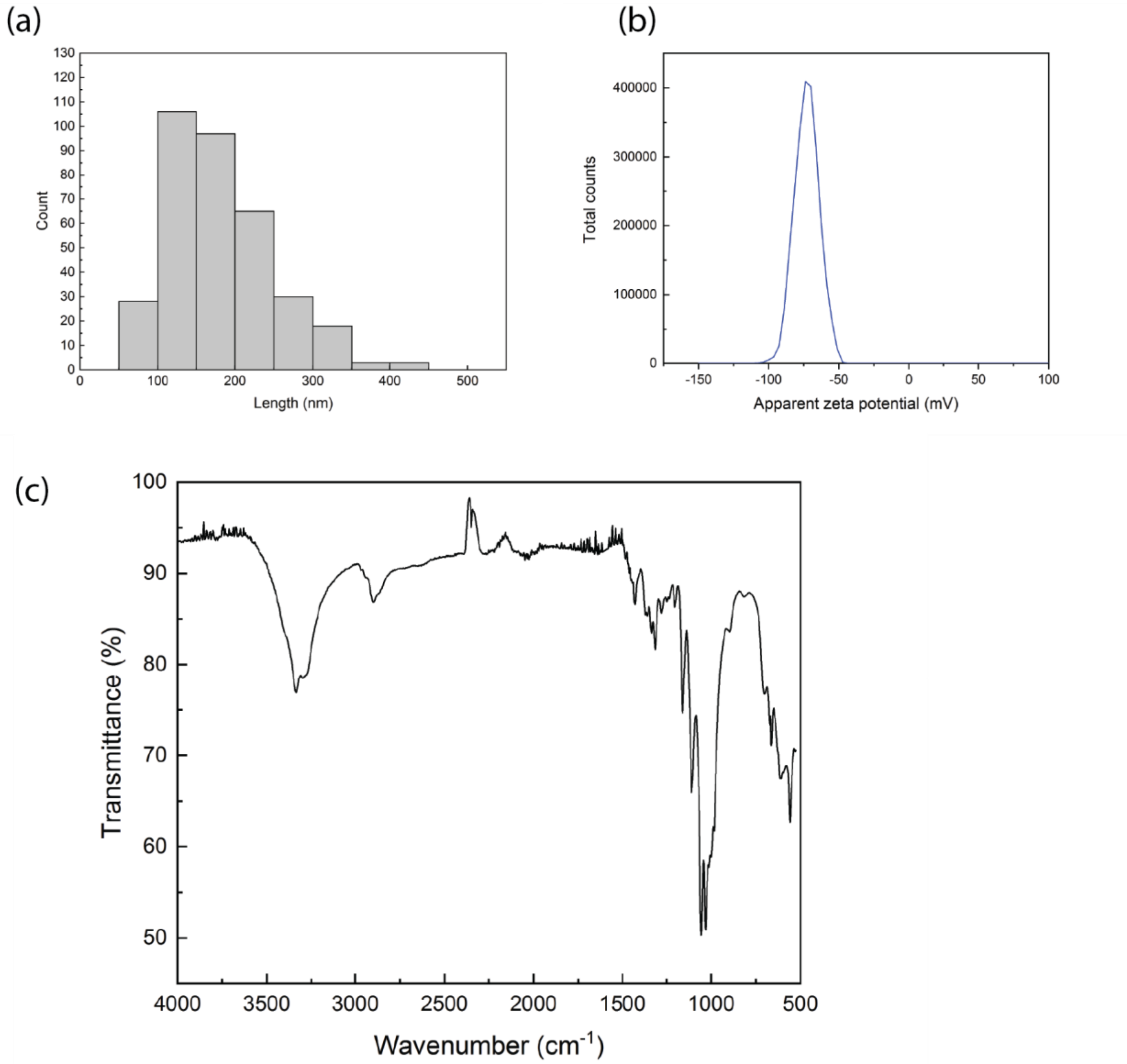

Figure S2. Characterization of CNC by TEM image analysis, DLS and FT-IR. The length distribution of CNC shown in (a) was calculated from TEM images to be 181 ± 69 nm (n =350). The zeta potential (b) was determined to be – 64 mV. in (c) FTIR spectrum of freeze-dried powder is shown. Note that the peaks between 2200 – 2400 cm^{-1} are due to measurement device and not from the sample.

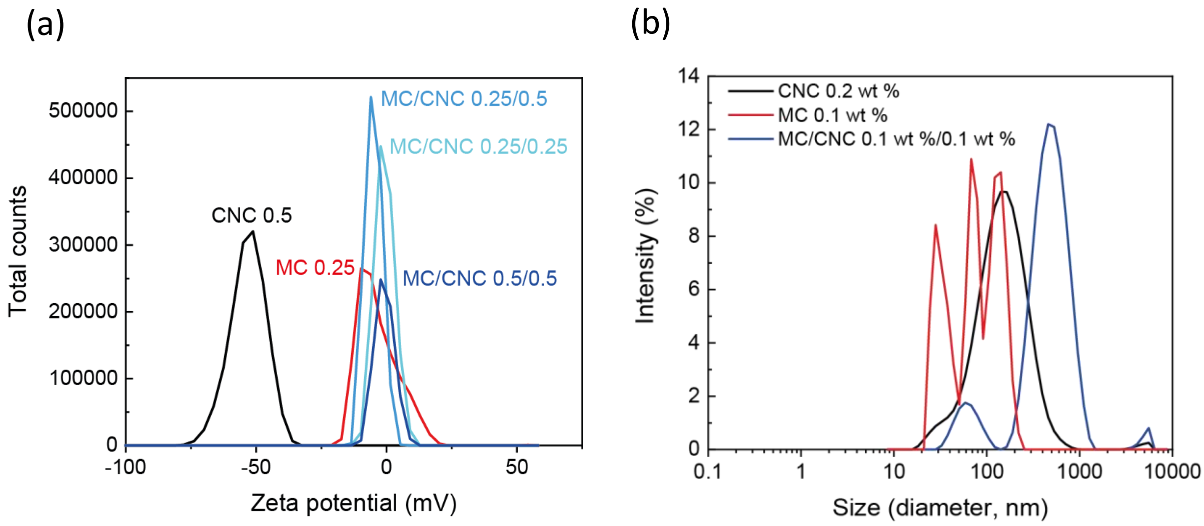

Figure S3. DLS size distribution and zeta potential of CNC, MC and MC/CNC mixtures. (a) Zeta potential distributions of 0.5 wt% CNC, 0.25 wt% MC, MC/CNC 0.25 wt% / 0.25 wt% and MC/CNC 0.25 wt% / 0.5 wt% show that while the zeta potential of pure CNC is highly negative, the pure MC and MC/CNC mixtures have only slightly negative and nearly neutral zeta potential. (b) Size distributions of the pure components and the mixtures show average particle diameter for 0.2 wt% CNC dispersion to be 164 nm, in the range of 20–150 nm with some polydispersity for 0.1 wt% MC and 459 nm for the MC/CNC 0.1 wt% / 0.1 wt% hybrids. Thus, no significant aggregation of the pure MC exists in the dispersions since the largest structures are formed from both MC and CNC.

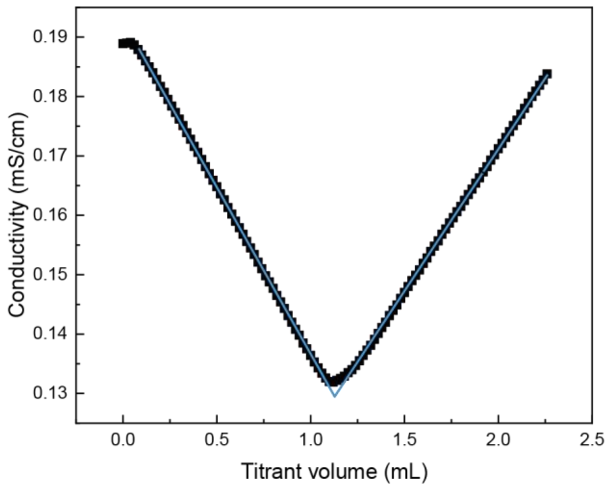

Figure S4. Conductometric titration curve of sulfuric acid hydrolyzed CNCs.

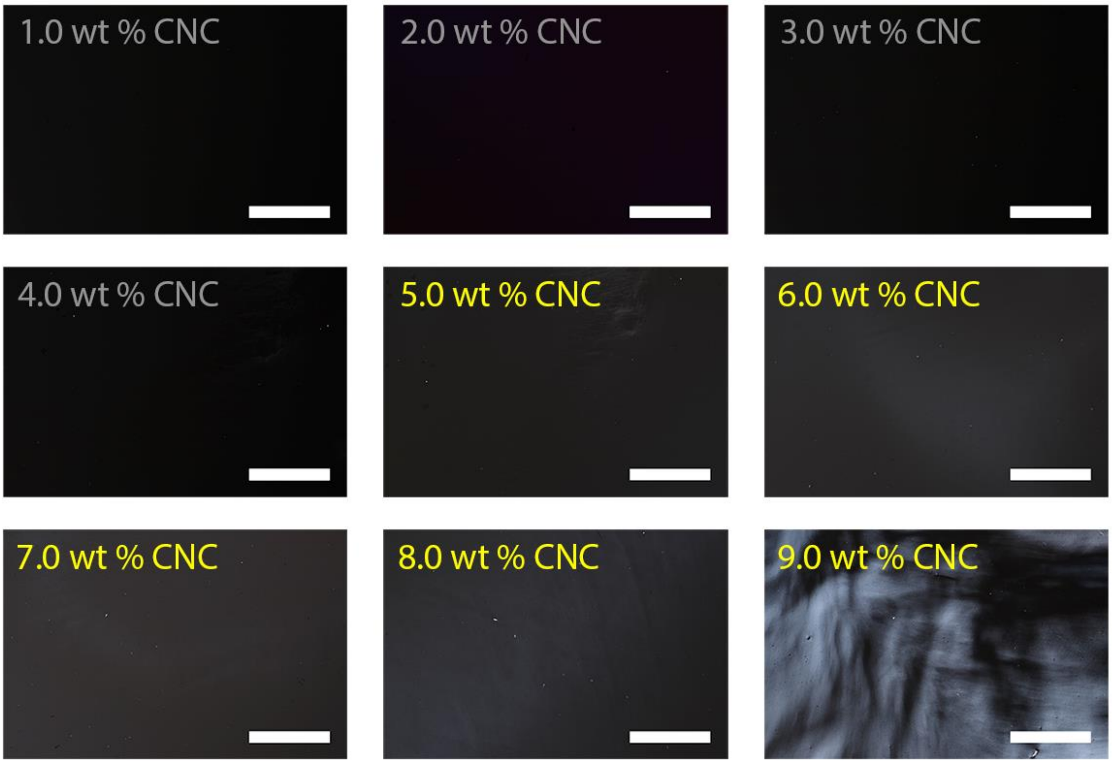

Figure S5. a) Polarized optical microscopy image of CNC dispersion ranging from 1.0 wt % to 9.0 wt % show the threshold concentration for liquid crystalline packing for the used CNCs is around 5.0 wt %. Concentrations where birefringence was detected are labelled with yellow text for clarity. Scale bars 1000 µm.

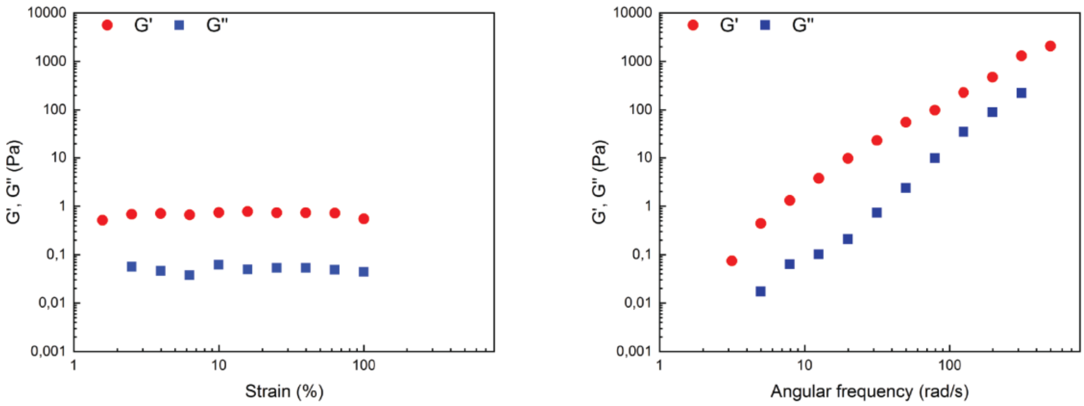

Figure S6. Strain and frequency sweeps of 3.5 wt% CNC dispersion at 20 °C. Strain sweeps were measured at an oscillation frequency of 6.283 rad/s and frequency sweeps at 1 % strain. Red circle corresponds to the storage modulus (*G*') and the blue square to the loss modulus (*G*'').

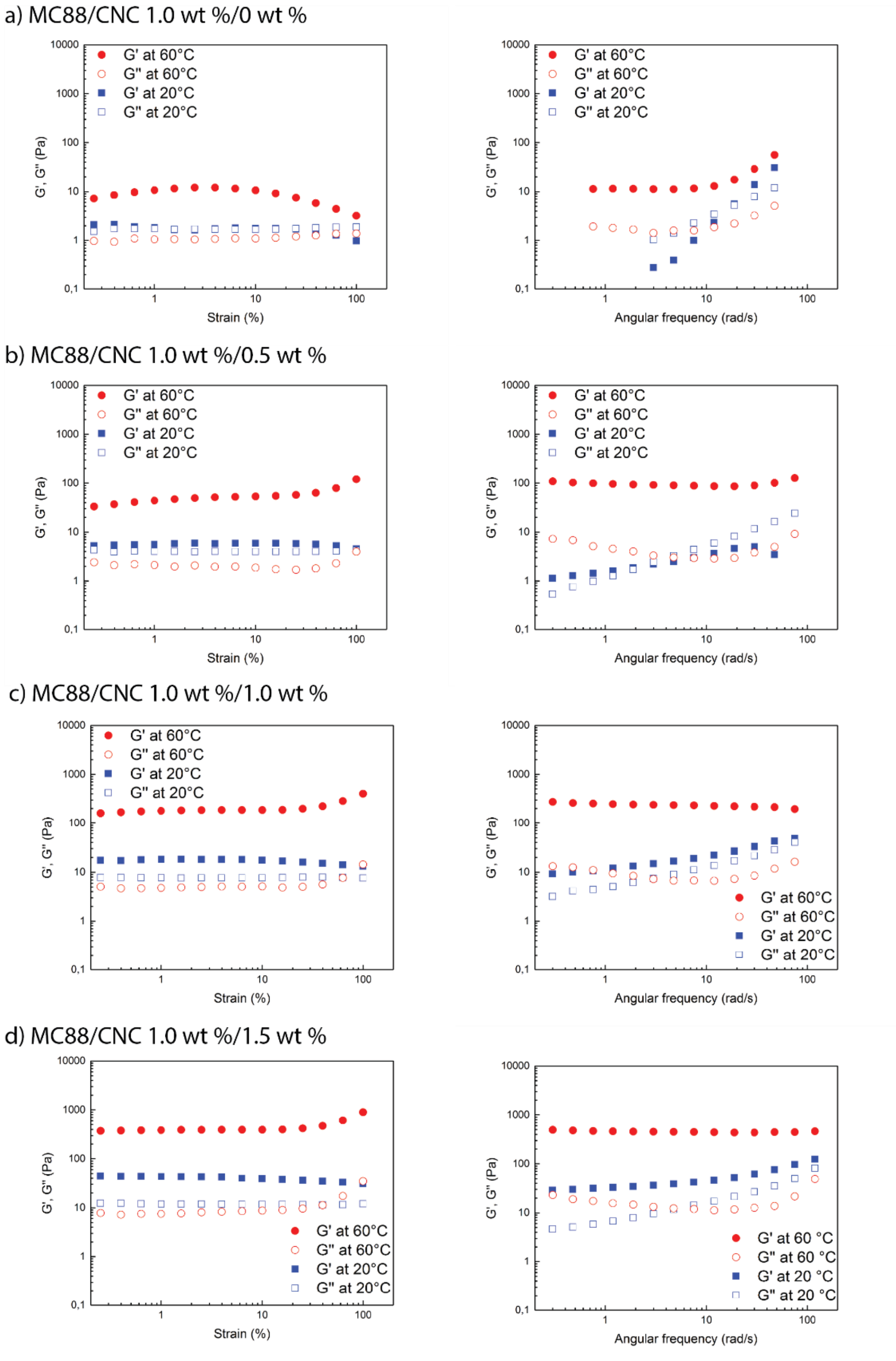
a) MC88/CNC 1.0 wt %/0 wt %
b) MC88/CNC 1.0 wt %/0.5 wt %
c) MC88/CNC 1.0 wt %/1.0 wt %
d) MC88/CNC 1.0 wt %/1.5 wt %
G' at 60°C
G'' at 60°C
G' at 20°C
G'' at 20°C
G' at 60 °C
G'' at 60 °C
G' at 20 °C
G'' at 20 °C
G', G'' (Pa)
Strain (%)
Angular frequency (rad/s)
10000
1000
100
10
1
0,1
1
10
100

e) MC88/CNC 1.0 wt %/2.0 wt %

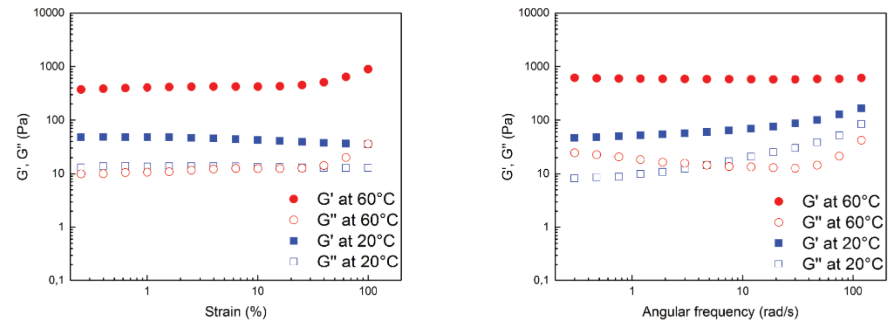

f) MC88/CNC 1.0 wt %/2.5 wt %

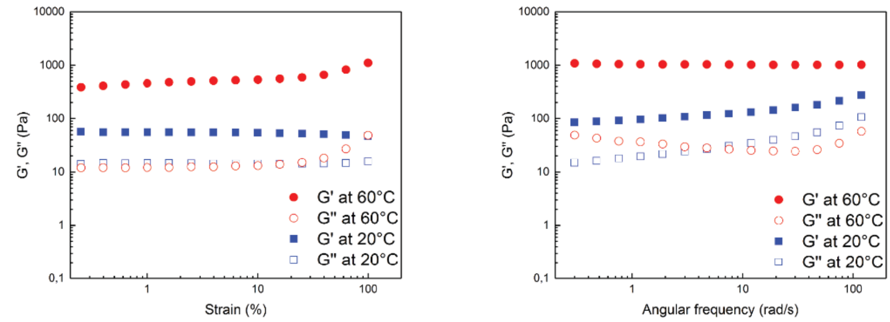

g) MC88/CNC 1.0 wt %/3.0 wt %

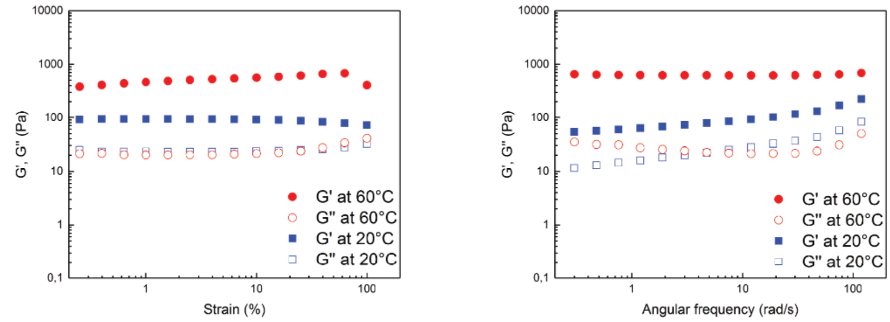

h) MC88/CNC 1.0 wt %/3.5 wt %

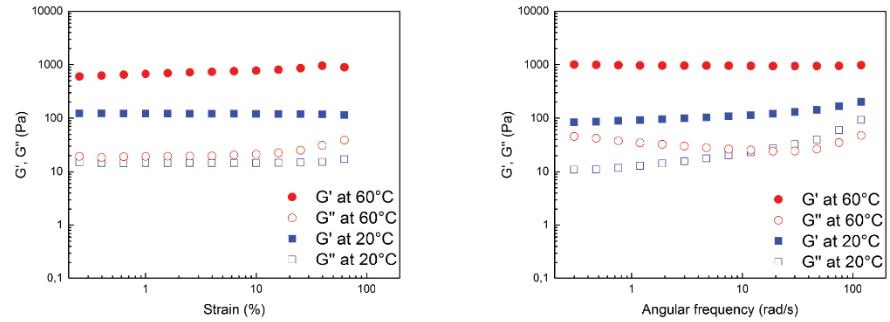

Figure S7. The strain sweeps (measured at 6.283 rad/s) and frequency sweeps (measured at 1 % strain) of MC88/CNC gels at various compositions measured at 20 °C and at 60 °C. For each graph: blue solid square represents *G*’ at 20 °C, blue open square *G*’’ at 20 °C, red solid circle *G*’ at 60 °C, and red open circle *G*’’ at 60 °C.

a) MC88/CNC 0.0 wt %/3.5 wt %

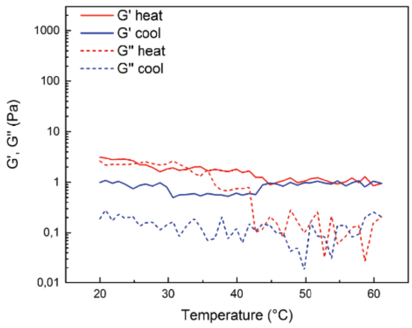

b) MC88/CNC 1.0 wt %/0.0 wt %

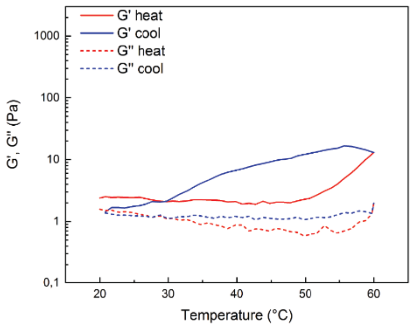

c) MC88/CNC 1.0 wt %/0.5 wt %

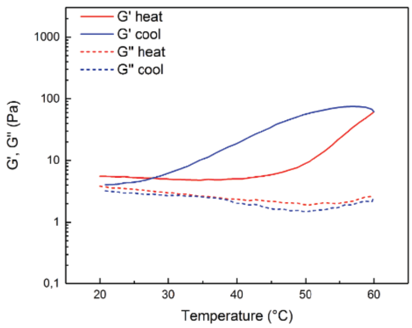

d) MC88/CNC 1.0 wt %/1.0 wt %

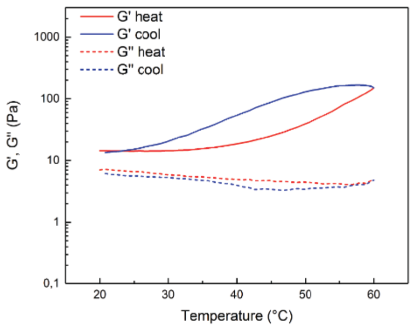

e) MC88/CNC 1.0 wt %/1.5 wt %

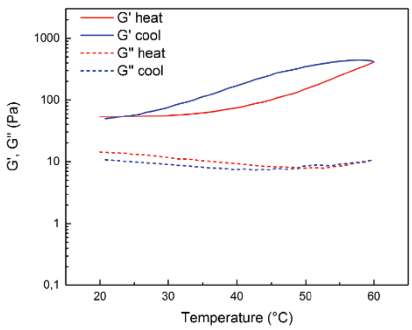

f) MC88/CNC 1.0 wt %/2.0 wt %

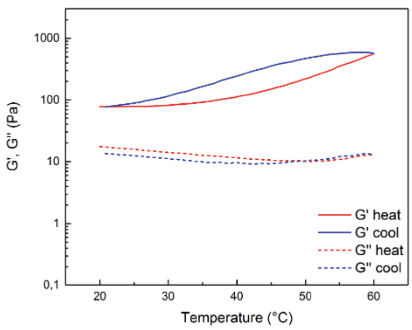

g) MC88/CNC 1.0 wt %/2.5 wt %

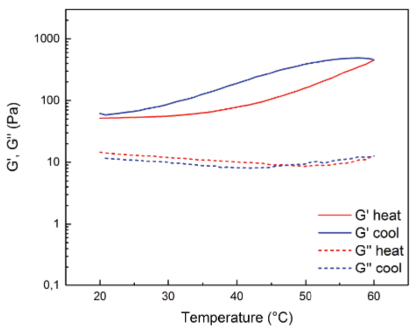

h) MC88/CNC 1.0 wt %/3.0 wt %

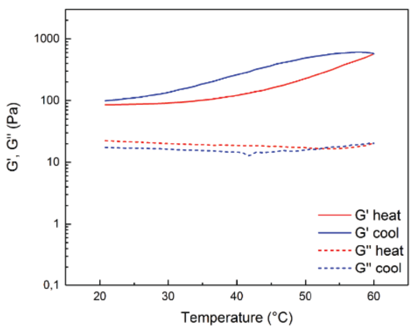

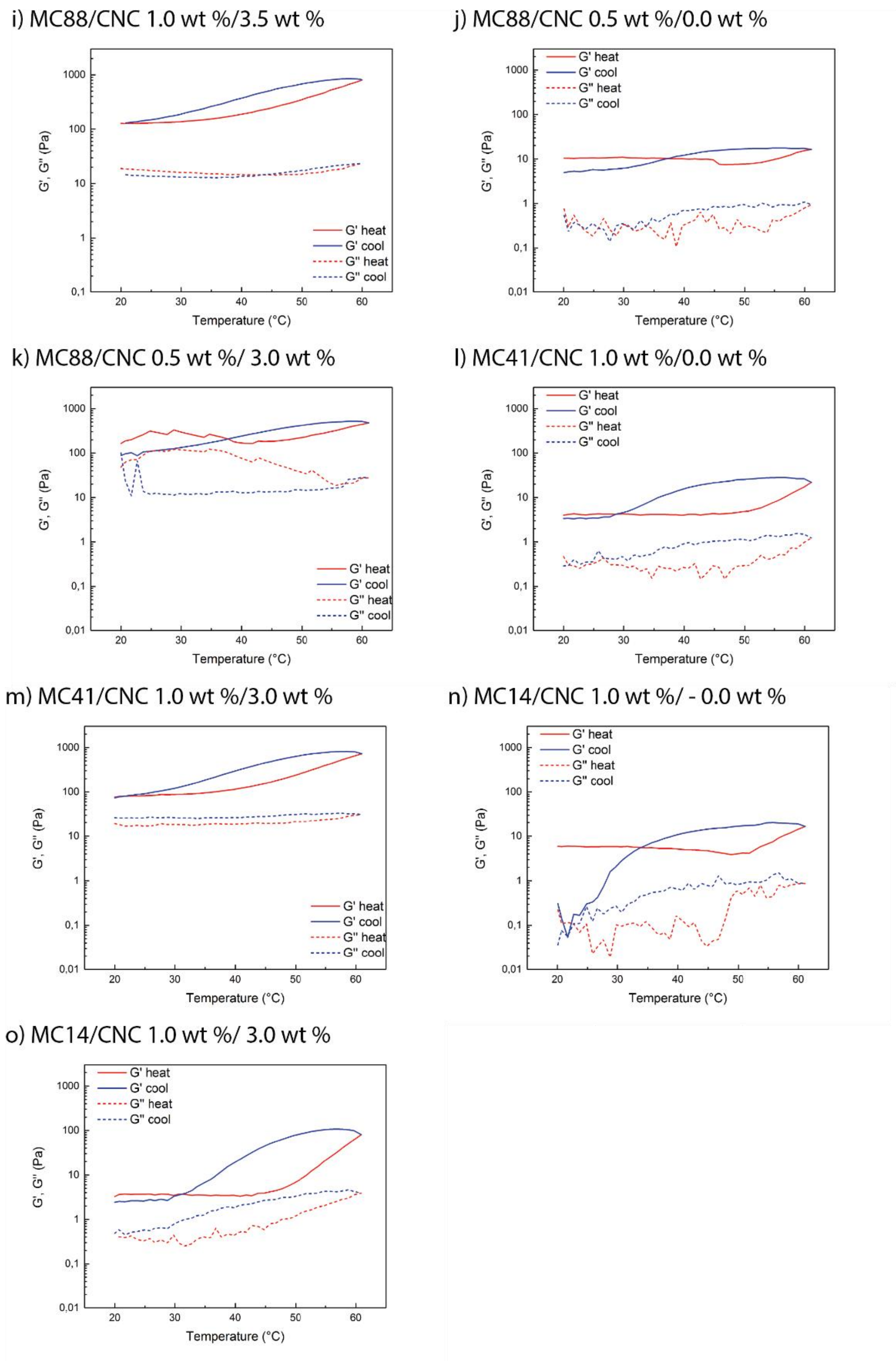

Figure S8. Temperature ramps of MC/CNC gels at various compositions. The gels were heated from 20 °C to 70 °C and then cooled back to 20 ° at a rate of 3 °C/min. *G*' and *G*'' were recorded at an angular frequency of 6.283 rad/s and 1 % strain. For each graph: solid line is *G*' and dashed line *G*''. Red line indicates the heating and blue the cooling phase of the experiment.

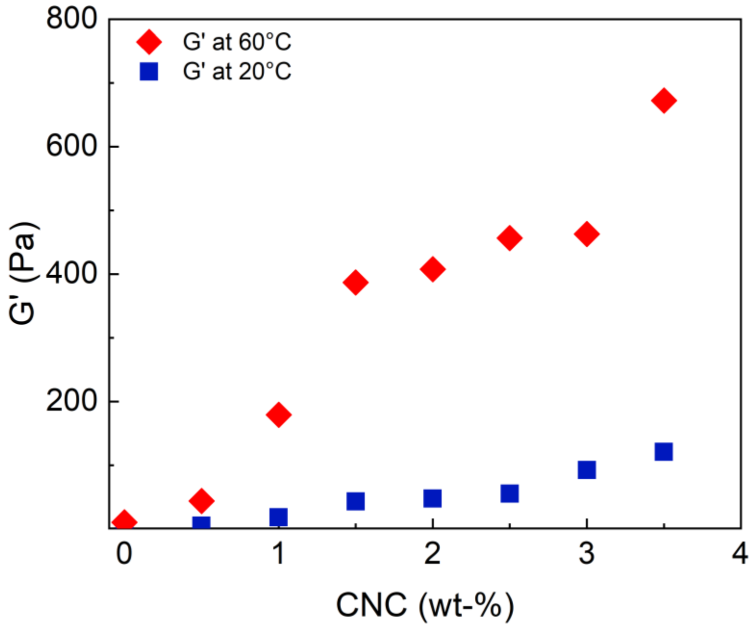

Figure S9. Storage modulus as a function of CNC concentration of MC/CNC hybrid gels when MC is fixed at 1 wt % at 20 °C and 60 °C.

a) MC88/CNC 0.5 wt %/0.0 wt %

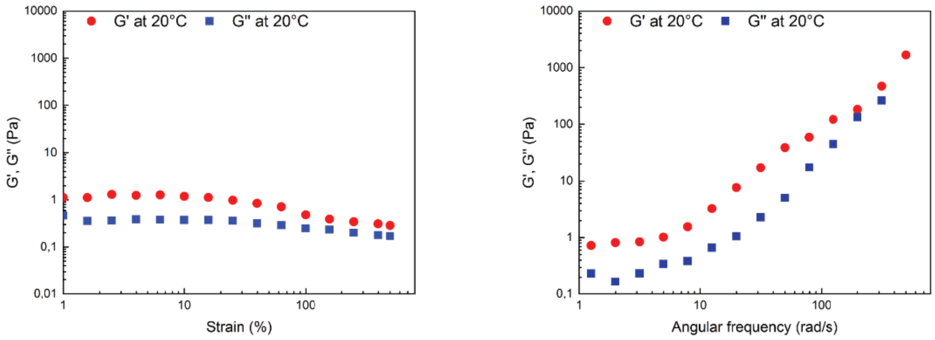

b) MC88/CNC 0.5 wt %/ 3.0 wt %

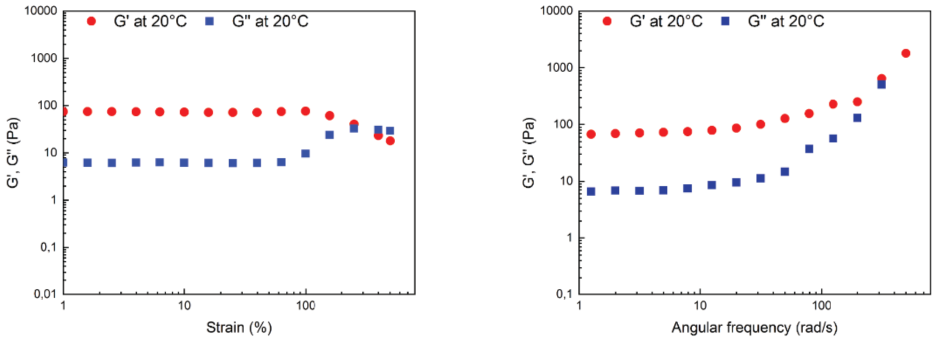

c) MC41/CNC 1.0 wt%/ 0.0 wt %

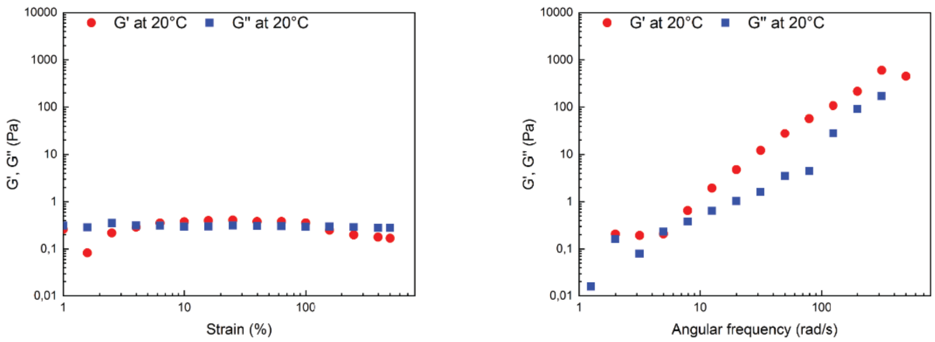

d) MC41/CNC 1.0 wt %/ 3.0 wt %

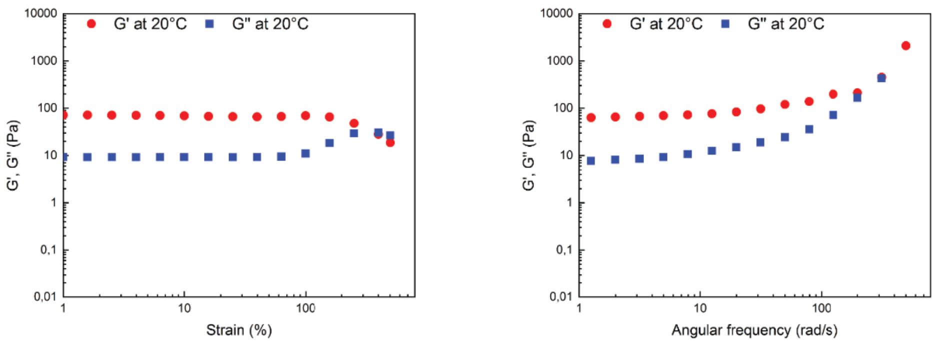

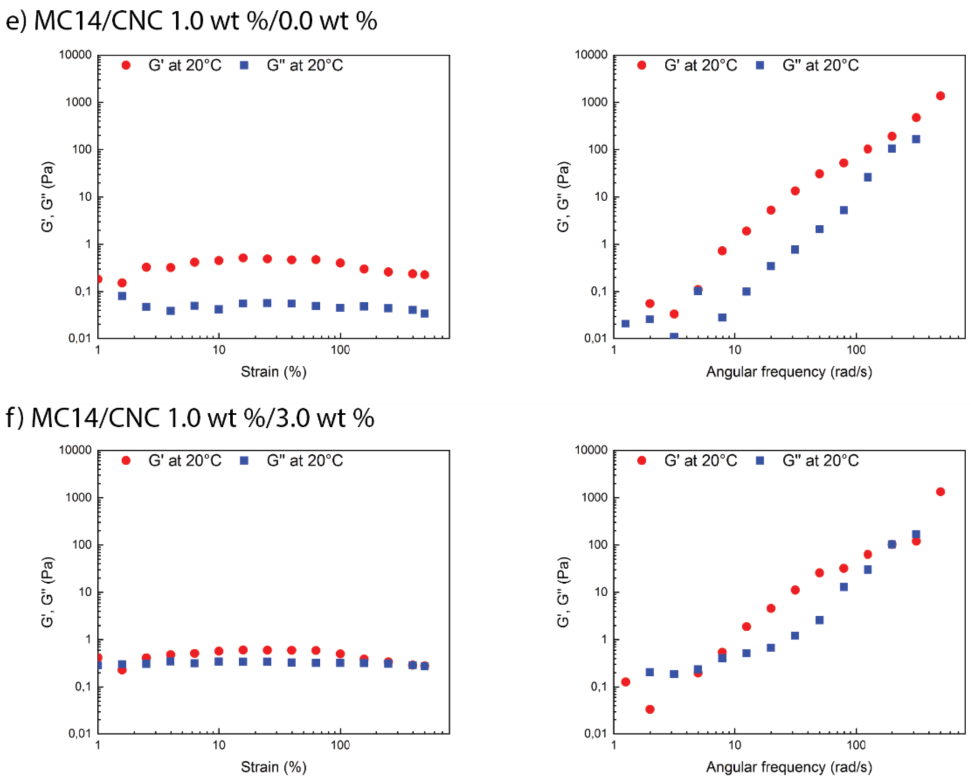

Figure S10. Reference strain sweeps (measured at 6.283 rad/s) and frequency sweeps (measured at 1 % strain) of MC-CNC hybrid gels with lower (0.5 wt %) MC88 concentration and with 1 wt % of two lower molecular weight MC (MC14 and MC41) at 20 °C. CNC concentration was either 0 or 3 wt %. For each graph: red solid circle is *G*' and blue solid square *G*''.

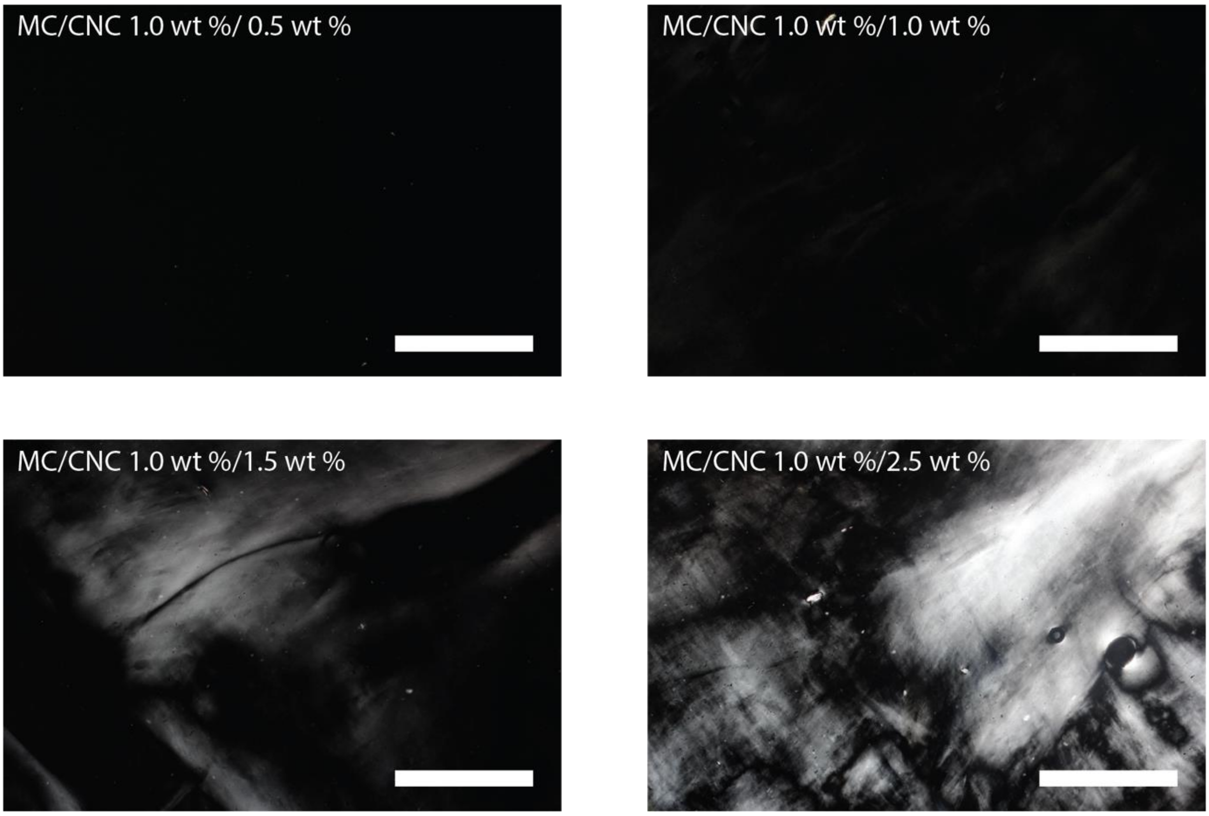

Figure S11. Birefringence intensity of MC88/CNC gels as a function of CNC concentration. Representative POM images are shown of MC88/CNC gels of various compositions. Scale bars 1 mm.

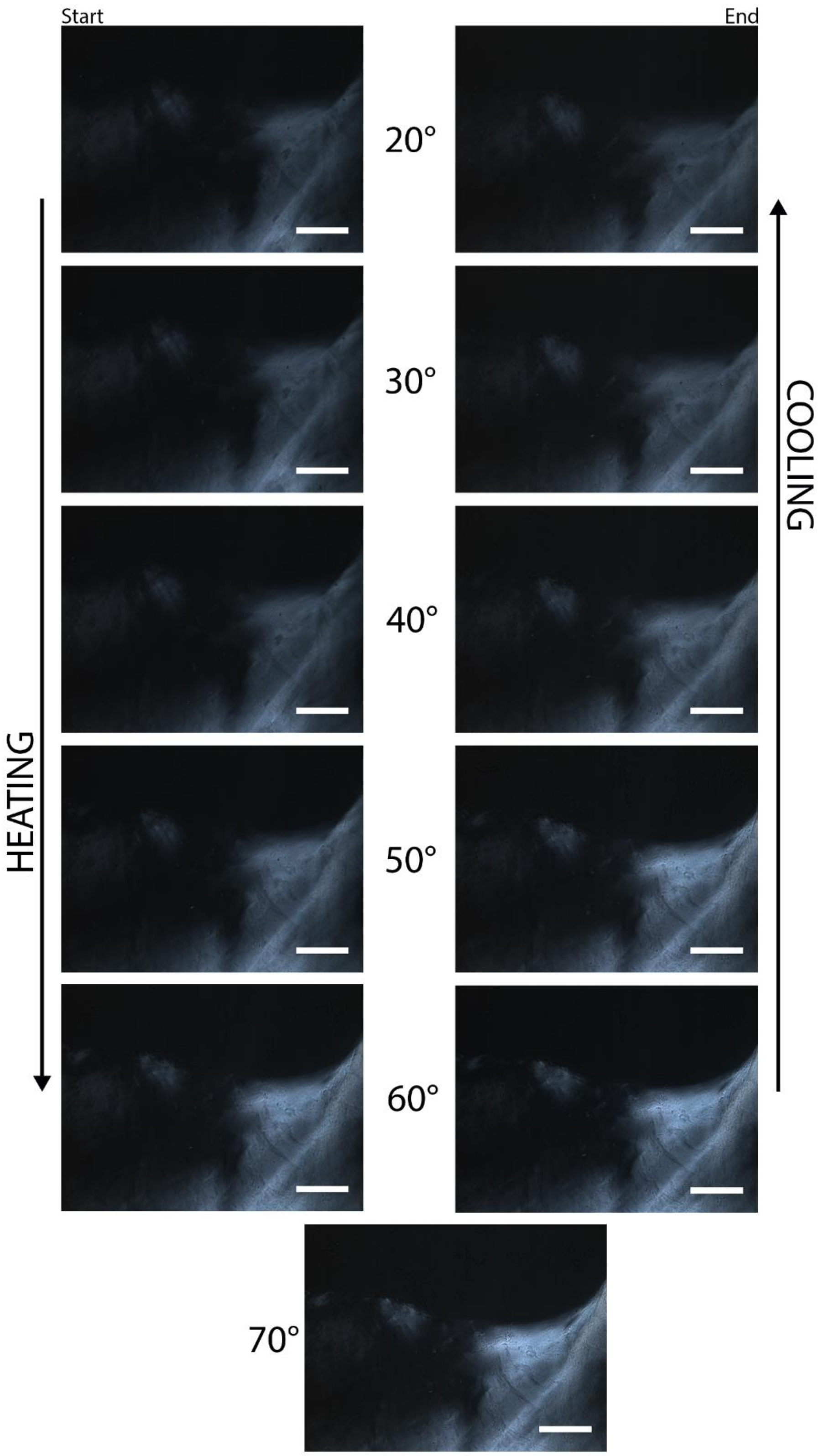

Figure S12. Representative POM image series of an MC88/CNC gel (1.0 wt%/2.5 wt%) during a 20 - 70 -20 °C temperature cycle. Scale bars 200 µm.

(a)
0.0 wt % MC88
3.5 wt % CNC

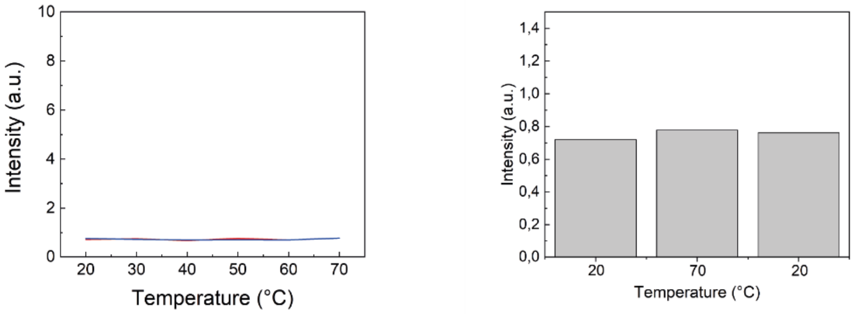

(b)
1.0 wt % MC88
0.0 wt % CNC

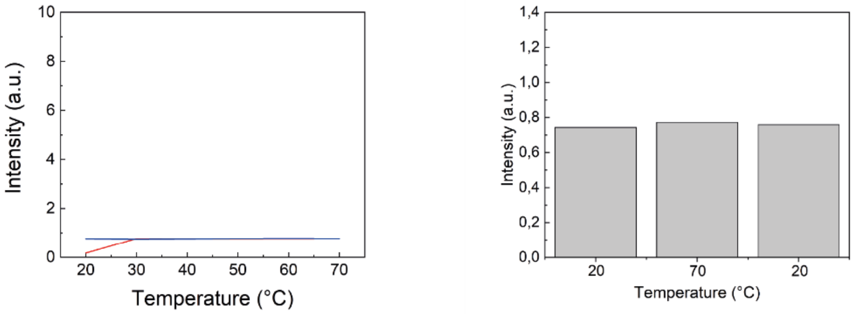

(c)
1.0 wt % MC88
0.5 wt % CNC

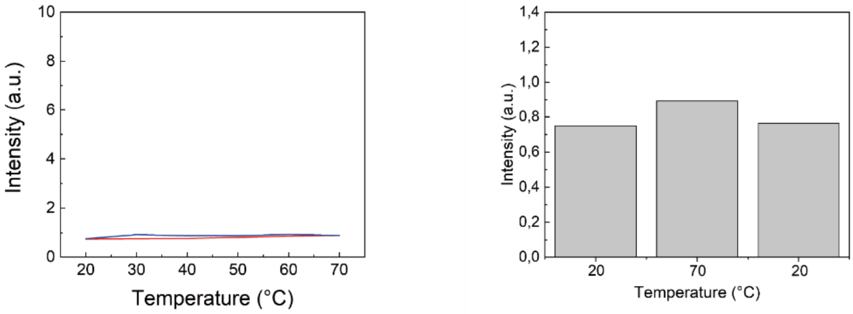

(d)
1.0 wt % MC88
1.0 wt % CNC

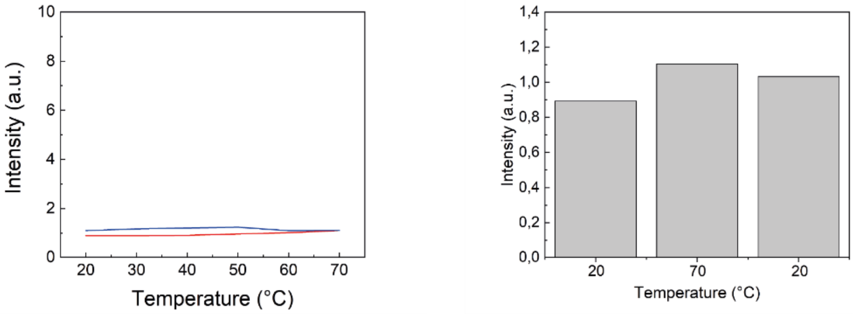

(e)
1.0 wt % MC88
1.5 wt % CNC

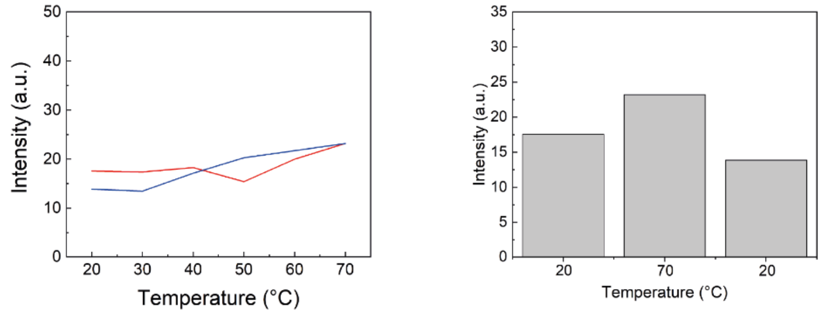

(f)
1.0 wt % MC88
2.0 wt % CNC

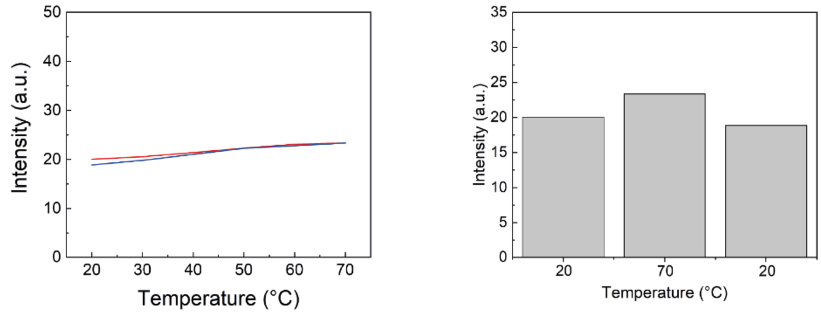

(g)
1.0 wt % MC88
2.5 wt % CNC

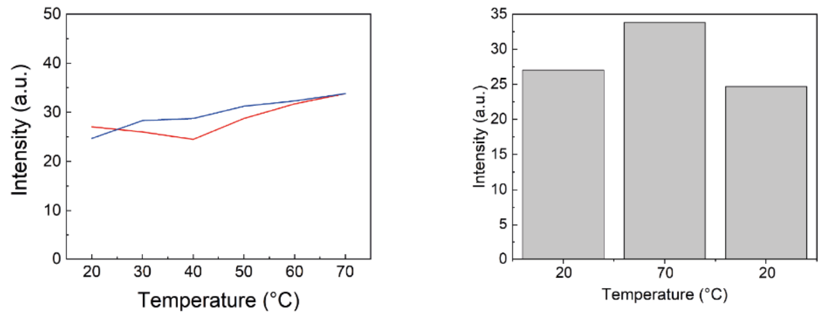

(h)
1.0 wt % MC88
3.0 wt % CNC

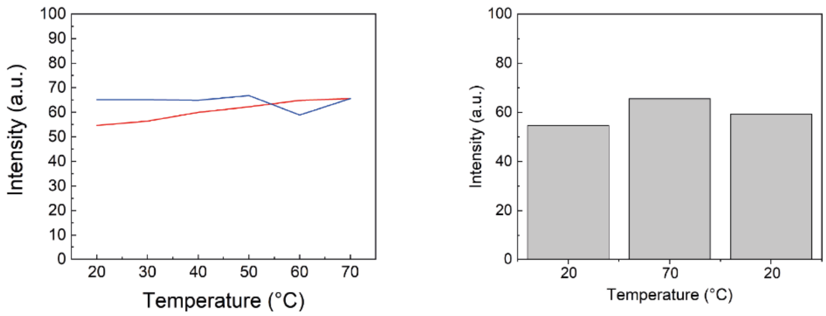

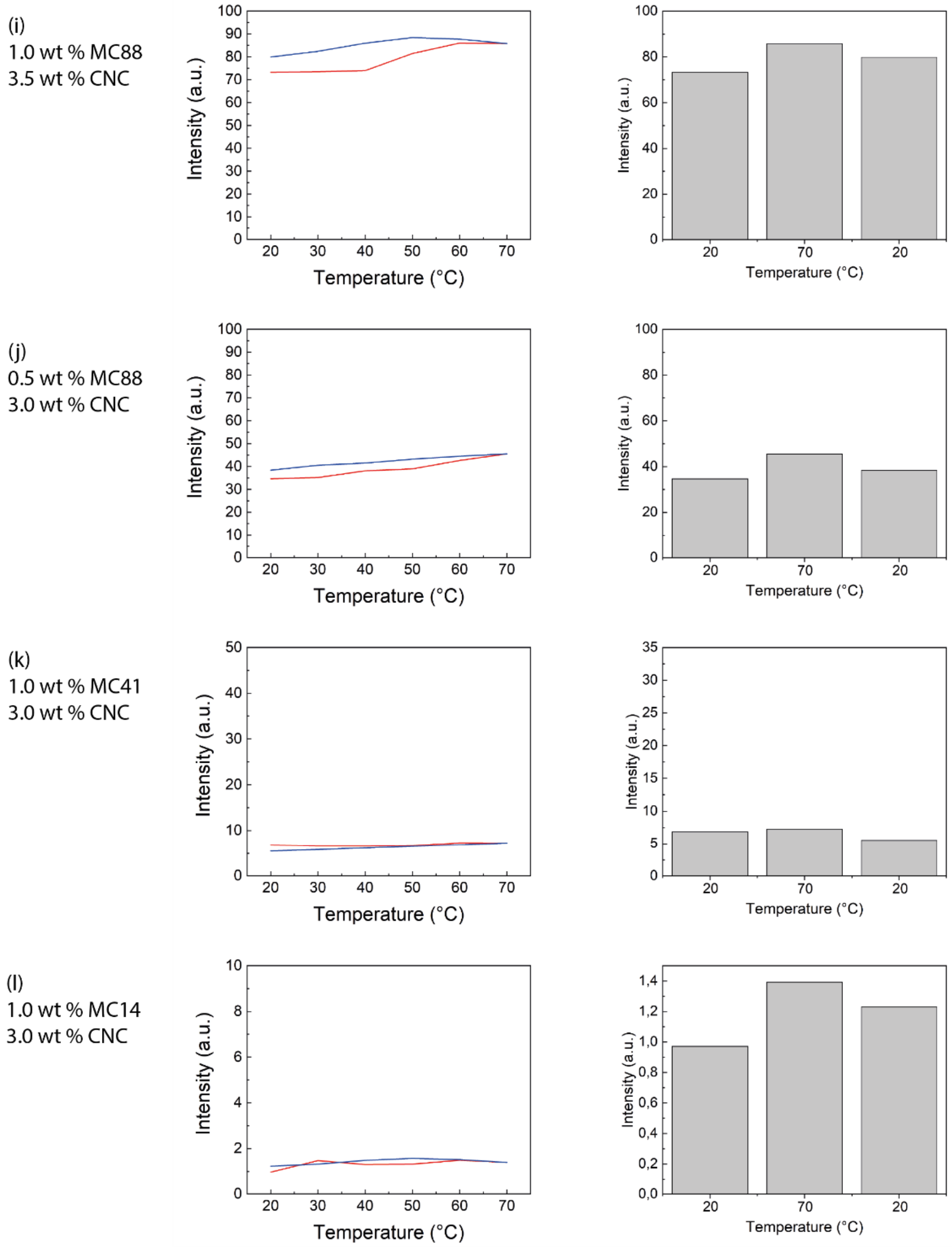

Figure S13. Birefringence intensity of MC/CNC gels at various compositions during the 20 – 70 – 20 °C temperature cycle. On the left, a representative intensity graph during the whole cycle (data points at every ten degrees) for each MC/CNC composition is depicted. On the right, the intensity values at the extremities of the cycle (20 °C at the beginning, 70 °C, and 20 °C at the end) are separately shown to highlight the observed change and reversibility.

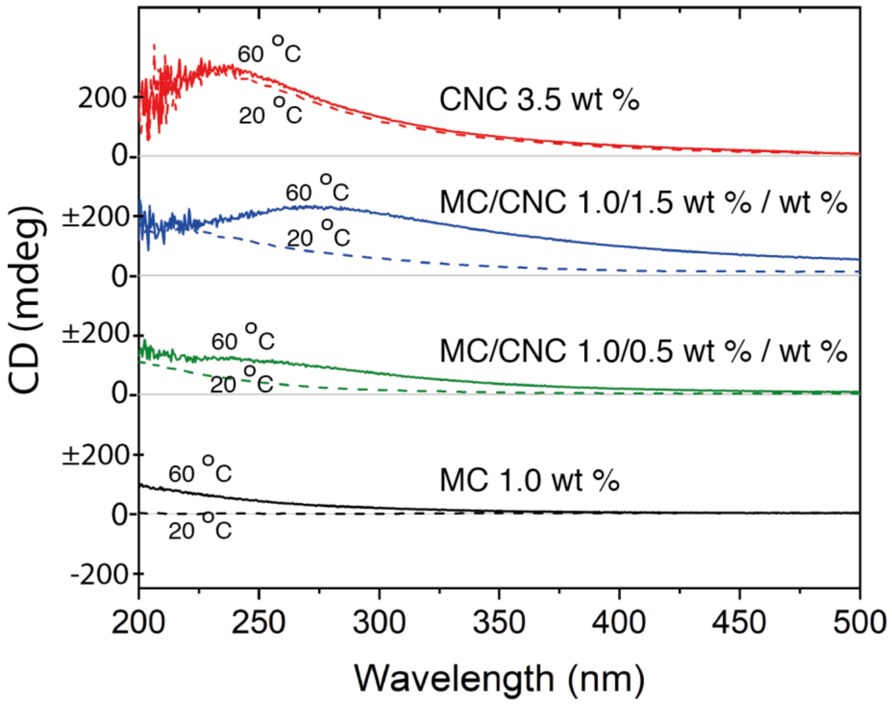

Figure S14. CD spectroscopy of MC88/CNC gels of different compositions at 20 °C and at 60 °C indicate a tendency for chirality and temperature driven peak shift (blue-shift of roughly ~50 – 100 nm;) indicative of structural changes in the chiral environment upon heating. No peak shift was observed with pure CNC (red). The CNC signal probably arises due to inherent chiral structure of CNCs or small chiral aggregates. Interestingly, even pure 1 wt % MC (black) gave chiral response when heated to 60 °C, not surprisingly based on the aggregation to the long fibers with ring-like lateral structures. However, the peak shift was only observed in mixtures where both components were present. Dashed line represents the measurement at 20 °C, and solid line at 60 °C. The gray solid lines indicate the zero-signal level for each sample. With CNC concentrations above 1.5 wt %, the gels became too opaque to be reliably measured.

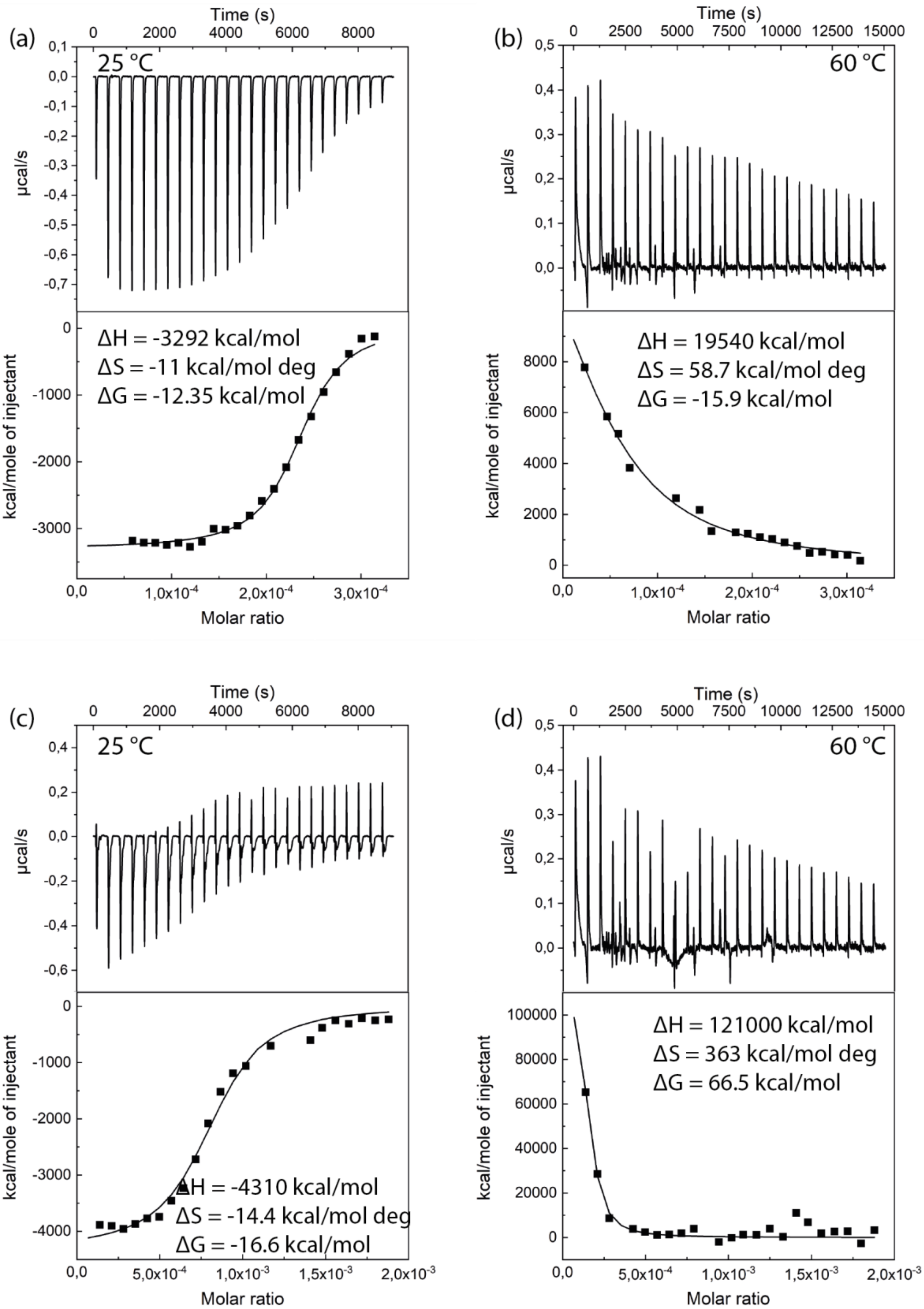

Figure S15. ITC titration curves and the extracted enthalpic (ΔH) and entropic (ΔS) contribution and the net Gibb's free energy change (ΔG) of the mixing of CNC with MC14 (a) at 25 °C and (b) at 60 °C, and with MC88 (c) at 25 °C and (d) at 60 °C.

References

(1) Elazzouzi-Hafraoui, S.; Nishiyama, Y.; Putaux, J.-L.; Heux, L.; Dubreuil, F.; Rochas, C. The Shape and Size Distribution of Crystalline Nanoparticles Prepared by Acid Hydrolysis of Native Cellulose. *Biomacromolecules* **2008**, *9* (1), 57–65.